

STRUCTURE PRESERVING MODEL REDUCTION OF PARAMETRIC HAMILTONIAN SYSTEMS

BABAK MABOUDI AFKHAM* AND JAN S. HESTHAVEN†

Abstract. While reduced-order models (ROMs) have been popular for efficiently solving large systems of differential equations, the stability of reduced models over long-time integration is of present challenges. We present a greedy approach for a ROM generation of parametric Hamiltonian systems that captures the symplectic structure of Hamiltonian systems to ensure stability of the reduced model. Through the greedy selection of basis vectors, two new vectors are added at each iteration to the linear vector space to increase the accuracy of the reduced basis. We use the error in the Hamiltonian due to model reduction as an error indicator to search the parameter space and identify the next best basis vectors. Under natural assumptions on the set of all solutions of the Hamiltonian system under variation of the parameters, we show that the greedy algorithm converges with exponential rate. Moreover, we demonstrate that combining the greedy basis with the discrete empirical interpolation method also preserves the symplectic structure. This enables the reduction of the computational cost for nonlinear Hamiltonian systems. The efficiency, accuracy, and stability of this model reduction technique is illustrated through simulations of the parametric wave equation and the parametric Schrödinger equation.

Key words. Symplectic model reduction, Hamiltonian system, Greedy basis generation, Symplectic Discrete Empirical Interpolation (SDEIM)

AMS subject classifications.

1. Introduction. Parameterized partial differential equations often arise as a model in many problems in engineering and the applied sciences. While the need for more accuracy has led to the development of exceedingly complex models, the limitations in computational cost and storage often make direct approaches impractical. Hence, we must seek alternative methods that allow us to approximate the desired output under variation of the input parameters while keeping the computational costs to a minimum.

Reduced basis methods have emerged as a powerful approach for the reduction of the intrinsic complexity of such models [22, 23, 24, 38]. These methods contain two stages: the offline stage and the online stage. In the offline stage, one explores the parameter space to construct a low-dimensional basis that accurately represents the parametrized solution to the partial differential equation. In this stage, the evaluation of the solution of the original model for multiple parameter values is required. The online stage comprises a Galerkin projection onto the span of the reduced basis, which allows exploration of the parameter space at a significantly reduced complexity [2, 21].

Convolutional reduced basis techniques, such as the Proper Orthogonal Decomposition (POD) [27, 3, 43], require the exploration of the entire parameter space. This leads to a very expensive and often impractical offline stage when dealing with multi-dimensional parameter domains. On the other hand, sampling techniques, usually of a greedy nature, search through the parameter space selectively, guided by an error estimate to certify the accuracy of the basis. This approach, accompanied with an efficient sampling procedure, balances the cost of computation with the overall accuracy of the reduced-basis [16, 44, 21].

Besides computational complexity, another aspect of reduced order modeling is

*Department of Mathematics, Chair of Computational Mathematics and Simulation Science (MCSS), École Polytechnique Fédérale de Lausanne, Switzerland (babak.maboudi@epfl.ch)

†Department of Mathematics, Chair of Computational Mathematics and Simulation Science (MCSS), École Polytechnique Fédérale de Lausanne, Switzerland (jan.hesthaven@epfl.ch)

the preservation of structure and, in particular, the stability of the original model. In general, reduced order models do not guarantee that such properties are preserved [41].

In the context of Hamiltonian and Lagrangian systems, recent work suggests modifications of POD to preserve some geometric structures. Lall et al. [28] and Carlberg et al. [12] suggests that the reduced-order system should be identified by a Lagrangian function on a low-dimensional configuration space. In this way, the geometric structure of the original system is inherited by the reduced system. Model reduction for port-Hamiltonian systems can be found in the works of Beattie et al. [14], Polyuga et al. [40] and references therein. These works construct a reduced port-Hamiltonian system using Krylov or POD methods that inherit the passivity and stability of the original system. For Hamiltonian systems, Peng et al. [37], using a symplectic transformation, constructs a reduced Hamiltonian, as an approximation to the Hamiltonian of the original system. As a result, the reduced system preserves the symplectic structure. Although these methods preserve the geometric structure, they use a POD-like approach for constructing the reduced basis. If the numerical evaluation of the original model is computationally demanding, performing POD can be excessively expensive [42].

In this paper, we present a greedy approach for the construction of a reduced system that preserves the geometric structure of Hamiltonian systems. This technique results in a reduced Hamiltonian system that mimics the symplectic properties of the original system and preserves the Hamiltonian structure and its stability over the course of time. On the other hand, since time integration of the original system is only required once per iteration, the proposed method saves substantial computational cost during the offline stage when compared to alternative POD-like approaches. It is well known that structured matrices, e.g. symplectic matrices, generally are not well-conditioned [25]. The greedy update of the symplectic basis presented here, yields a orthosymplectic basis and, therefore, a norm bounded basis. Moreover, we demonstrate that assumptions, natural for the set of all solutions of the original Hamiltonian system under variation of parameters, lead to exponentially fast convergence of the greedy algorithm. For nonlinear Hamiltonian systems, we show how the basis can be combined with the discrete empirical interpolation method (DEIM) [15, 4] to enable a fast evaluation of nonlinear terms while maintaining the symplectic structure.

This paper is organized as follows. Section 2 presents a brief overview of model order reduction, POD and DEIM. In Section 3 we cover the required topics from symplectic geometry and Hamiltonian systems. Section 4 discusses the greedy generation of a symplectic reduced basis as well as other SVD-based symplectic model reduction techniques. Accuracy, stability, and efficiency of the greedy method compared to other SVD-based methods are discussed in Section 5. Finally we offer some conclusive remarks in Section 6.

2. Model Order Reduction. Consider a parameterized, finite dimensional dynamical system described by a set of first order ordinary differential equations

$$(1) \quad \begin{cases} \frac{d}{dt}\mathbf{x}(t, \omega) = \mathbf{f}(t, \mathbf{x}, \omega), \\ \mathbf{x}(0, \omega) = \mathbf{x}_0(\omega). \end{cases}$$

Here $\mathbf{x} \in \mathbb{R}^n$ is the state vector, $\omega \in \Gamma$ is a vector containing all the parameters of the system belonging to a compact set $\Gamma \subset \mathbb{R}^d$ and $\mathbf{f} : \mathbb{R} \times \mathbb{R}^n \times \Gamma \rightarrow \mathbb{R}^n$ is a general vector valued function of the state variables and parameters.

We define the solution manifold as the set of all solutions to (1) under variation of the parameters in Γ

$$(2) \quad \mathcal{M} = \{\mathbf{x}(t, \omega) | \omega \in \Gamma, t \geq 0\} \subset \mathbb{R}^n.$$

Note that the exact solution and solution manifold is often not available; we assume that we have a numerical integrator that can approximate the solution to (1) for any realization of ω with a given accuracy. By abuse of notation, we refer to \mathbf{x} and \mathcal{M} as the exact solution and the exact solution manifold, respectively, rather than the discrete solution and discrete solution manifold.

Model order reduction is based on the assumption that \mathcal{M} is of low dimension [21, 2] and that the span of appropriately chosen basis vectors $\{v_i\}_{i=1}^k$ covers most of the solution manifold to within a small error. The set $\{v_i\}_{i=1}^k$ is denoted as the *reduced basis* and its span as the *reduced space*. Assuming that a k -dimensional ($k \ll n$) reduced basis is given, the approximated solution can be represented as

$$(3) \quad \mathbf{x} \approx V\mathbf{y},$$

where V is a matrix containing the reduced basis vectors as its columns and \mathbf{y} contains the coordinates of the approximation in this basis. By substituting (3) into (1) we obtain the overdetermined system

$$(4) \quad V \frac{d}{dt} \mathbf{y} = \mathbf{f}(t, V\mathbf{y}, \omega) + \mathbf{r}(t, \omega).$$

Here we added the residual \mathbf{r} to emphasize that (4) is an approximation of (1). Taking the Petrov-Galerkin projection [2] we construct a basis W of size $n - k$ that is orthogonal to the residual \mathbf{r} and requires that $W^T V$ is invertible. This yields

$$(5) \quad \frac{d}{dt} \mathbf{y} = (W^T V)^{-1} \mathbf{f}(t, V\mathbf{y}, \omega).$$

Equation (5) consists of k equations and is called the reduced system. Solving the reduced system instead of the original system can reduce the computational costs provided k is significantly smaller than n . For nonlinear systems, the evaluation of \mathbf{f} may still have computational complexity that depends on n . We return to this question in detail in Section 2.2.

2.1. Proper Orthogonal Decomposition. Let $\mathbf{x}(t_i, \omega_j)$ with $i = 1, \dots, m$ and $j = 1, \dots, n$ be a finite number of samples, referred to as *snapshots*, from the solution manifold (2). If we assume that a reduced basis V is provided, the projection operator from \mathbb{R}^n onto the reduced space can be constructed as VV^T . The proper orthogonal decomposition (POD) requires the total error of projecting all the snapshots onto the reduced space to be minimized. The POD basis of size k is thus the solution to the optimization problem

$$(6) \quad \begin{aligned} & \underset{V \in \mathbb{R}^{n \times k}}{\text{minimize}} && \|S - VV^T S\|_F \\ & \text{subject to} && V^T V = I_k \end{aligned}$$

Here S is the snapshot matrix, containing snapshots $\mathbf{x}(t_i, \omega_j)$ in its columns, $\|\cdot\|_F$ is the Frobenius norm and I_k is the identity matrix of size k . According to the Schmidt-Mirsky-Eckart-Young theorem [29], the solution to (6) is equivalent to the truncated singular value decomposition (SVD) of the snapshot matrix S given by

$$(7) \quad V = \sigma_1 u_1 v_1^T + \dots + \sigma_k u_k v_k^T.$$

Here σ_i , u_i and v_i are the singular values, the left singular vectors, and the right singular vectors of S , respectively [29].

2.2. Discrete Empirical Interpolation Method (DEIM). In this section we discuss the efficiency of evaluating nonlinearities in the context of projection based reduced models. Suppose that the right hand side in (1) is of the form $\mathbf{f}(t, \mathbf{x}, \omega) = L\mathbf{x} + \mathbf{g}(t, \mathbf{x}, \omega)$, where $L \in \mathbb{R}^{n \times n}$ reflects the linear part, and \mathbf{g} is a nonlinear function. Now assume that a k -dimensional reduced basis V is provided. The reduced system takes the form

$$(8) \quad \frac{d}{dt}\mathbf{y} = \underbrace{(W^T V)^{-1} L V}_{\tilde{L}} \mathbf{y} + \underbrace{(W^T V)^{-1} \mathbf{g}(t, V\mathbf{y}, \omega)}_{\tilde{N}(\mathbf{y})}.$$

Here, \tilde{L} is a $k \times k$ matrix which can be computed before time integration of the reduced system. However, the evaluation of $\tilde{N}(\mathbf{y})$ has a complexity that depends on n , the size of the original system. Suppose that the evaluation of \mathbf{g} with n components has the complexity $\alpha(n)$, for some function α . Then the complexity of evaluating $\tilde{N}(\mathbf{y})$ is $\mathcal{O}(\alpha(n) + 4nk)$ which consists of 2 matrix-vector operations and the evaluation of the nonlinear function, i.e. the evaluation of the nonlinear terms can be as expensive as solving the original system.

To overcome this bottleneck we take an approach similar to that of Section 2.1 [15, 4]. Assume that the manifold $\mathcal{M}_{\mathbf{g}} = \{\mathbf{g}(t, \mathbf{x}, \omega) | t \in \mathbb{R}, \mathbf{x} \in \mathbb{R}, \omega \in \Gamma\}$ is of a low dimension and that \mathbf{g} can be approximated by a linear subspace of dimension $m \ll n$, spanned by the basis $\{u_1, \dots, u_m\}$, i.e.

$$(9) \quad \mathbf{g}(t, \mathbf{x}, \omega) \approx U\mathbf{c}(t, \mathbf{x}, \omega).$$

Here U contains basis vectors u_i and \mathbf{c} is the vector of coefficients. Now suppose p_1, \dots, p_m are m indices from $\{1, \dots, n\}$ and define an $n \times m$ matrix

$$(10) \quad P = [e_{p_1}, \dots, e_{p_m}],$$

where e_{p_i} is the p_i -th column of the identity matrix I_n . Multiplying P with \mathbf{g} selects components p_1, \dots, p_m of \mathbf{g} . If we assume that $P^T U$ is non-singular, the coefficient vector \mathbf{c} can be uniquely determined from

$$(11) \quad P^T \mathbf{g} = (P^T U)\mathbf{c}.$$

Finally the approximation of \mathbf{g} is determined by

$$(12) \quad \mathbf{g}(t, \mathbf{x}, \omega) \approx U\mathbf{c}(t, \mathbf{x}, \omega) = U(P^T U)^{-1} P^T \mathbf{g}(t, \mathbf{x}, \omega),$$

which is referred to as the *Discrete Empirical Interpolation* (DEIM) approximation [15]. Applying DEIM to the reduced system (5) yields

$$(13) \quad \frac{d}{dt}\mathbf{y} = \tilde{L}\mathbf{y} + (W^T V)^{-1} U(P^T U)^{-1} P^T \mathbf{g}(t, V\mathbf{y}, \omega).$$

Note that the matrix $(WV)^{-1} U(P^T U)^{-1}$ can be computed offline and since \mathbf{g} is evaluated only at m of its components, the evaluation of the nonlinear term in (13) does not depend on n .

To obtain the projection basis U , the POD can be applied to the ensemble of samples of the nonlinear term $\mathbf{g}(t_i, \mathbf{x}, \omega_j)$ with $i = 1, \dots, m$ and $j = 1, \dots, n$. There

is no additional cost associated with computing the nonlinear snapshots, since they are generated when computing the trajectory snapshot matrix S . The interpolating indices p_1, \dots, p_m can be constructed as follows. Given the projection basis $U = \{u_1, \dots, u_m\}$, the first interpolation index p_1 is chosen according to the component of u_1 with the largest magnitude. The rest of the interpolation indices, p_2, \dots, p_m correspond to the component of the largest magnitude of the residual vector $\mathbf{r} = u_l - U\mathbf{c}$. It is shown in [15] that if the residual vector is a nonzero vector in each iteration then $P^T U$ is non-singular and (12) is well defined.

Algorithm 1 Discrete Empirical Interpolation Method

Input: Basis vectors $\{u_1, \dots, u_m\} \subset \mathbb{R}^n$

1. pick p_1 to be the index of the largest component of u_1 .
2. $U \leftarrow [u_1]$
3. $P \leftarrow [p_1]$
4. **for** $i \leftarrow 2$ **to** m
5. solve $(P^T U)\mathbf{c} = P^T u_i$ for \mathbf{c}
6. $\mathbf{r} \leftarrow u_i - U\mathbf{c}$
7. pick p_i to be the index of the largest component of \mathbf{r}
8. $U \leftarrow [u_1, \dots, u_i]$
9. $P \leftarrow [p_1, \dots, p_i]$
10. **end for**

Output: Interpolating indices $\{p_1, \dots, p_m\}$

The numerical solution of (8) may involve the computation of the Jacobian of the nonlinear function $\mathbf{g}(t, \mathbf{x}, \omega)$ with respect to the reduced state variable \mathbf{y}

$$(14) \quad \mathbf{J}_{\mathbf{y}}(\mathbf{g}) = (W^T V)^{-1} \mathbf{J}_{\mathbf{x}}(\mathbf{g}) V,$$

where $\mathbf{J}_{\alpha}(\mathbf{g})$ is the Jacobian matrix of \mathbf{g} with respect to the variable α . The complexity of (14) is $\mathcal{O}(\alpha(n) + 2n^2k + 2nk^2 + 2nk)$, comprising several matrix-vector multiplications and an evaluation of the Jacobian which depends on the size of the original system. Approximating the Jacobian in (14) is usually both problem and discretization dependent. Often the nonlinear function \mathbf{g} is evaluated component-wise i.e.

$$(15) \quad \mathbf{g}(\mathbf{x}) = \begin{pmatrix} g_1(x_1, \dots, x_n) \\ g_2(x_1, \dots, x_n) \\ \vdots \\ g_n(x_1, \dots, x_n) \end{pmatrix} = \begin{pmatrix} g_1(x_1) \\ g_2(x_2) \\ \vdots \\ g_n(x_n) \end{pmatrix}.$$

In such cases the interpolating index matrix P and the nonlinear function \mathbf{g} commute, i.e.,

$$(16) \quad \tilde{N}(\mathbf{y}) \approx (W^T V)^{-1} U (P^T U)^{-1} P^T \mathbf{g}(V\mathbf{y}) = (W^T V)^{-1} U (P^T U)^{-1} \mathbf{g}(P^T V\mathbf{y})$$

If we now take the Jacobian of the approximate function we recover

$$(17) \quad \mathbf{J}_{\mathbf{y}}(\mathbf{g}) = \underbrace{(W^T V)^{-1} U (P^T U)^{-1}}_{k \times m} \underbrace{\mathbf{J}_{\mathbf{x}}(\mathbf{g}(P^T V\mathbf{y}))}_{m \times m} \underbrace{P^T V}_{m \times k}.$$

The matrix $(WV)^{-1}U(P^TU)^{-1}$ can be computed offline and the Jacobian is evaluated only for $m \times m$ components. Hence the overall complexity of computing the Jacobian is now independent of n . We refer the reader to [4, 15] for more detail.

3. Hamiltonian Systems and Symplectic Geometry. Let \mathcal{M} be a manifold and $\Omega : \mathcal{M} \times \mathcal{M} \rightarrow \mathbb{R}$ be a closed, nondegenerate and skew-symmetric 2-form on \mathcal{M} . The pair (\mathcal{M}, Ω) is called a *symplectic manifold* [30].

Let (\mathcal{M}, Ω) be a symplectic manifold and suppose that $H : \mathcal{M} \rightarrow \mathbb{R}$ is a smooth scalar function. The differential of H , denoted by $\mathbf{d}H$, defines a 1-form on \mathcal{M} . The nondegeneracy of Ω implies that there is a unique vector field X_H , the *Hamiltonian vector field* [17, 30], on \mathcal{M} such that

$$(18) \quad i_{X_H} \Omega = \mathbf{d}H.$$

Here $i_{X_H} \Omega$ is the interior product of X_H with Ω , i.e.,

$$(19) \quad \Omega(X_H, Y) = \mathbf{d}H(Y),$$

for any vector field Y on \mathcal{M} . Note that when \mathcal{M} belongs to a Euclidean space then $\mathbf{d}H = \nabla_z H$. The equations of evolution are then defined by

$$(20) \quad \dot{z} = X_H(z)$$

and known as *Hamilton's equation* [30]. A fundamental feature of Hamiltonian systems is the conservation of the Hamiltonian along integral curves on \mathcal{M} . To emphasize the importance of this property we recall [30]

THEOREM 1. *Suppose that X_H is a Hamiltonian vector field with the flow ϕ_t on a symplectic manifold \mathcal{M} . Then $H \circ \phi_t = H$.*

Proof. H is constant along integral curves since

$$(21) \quad \begin{aligned} \frac{d}{dt}(H \circ \phi_t)(z) &= \mathbf{d}H(\phi_t(z)) \cdot \left(\frac{d}{dt}\phi_t(z)\right) \\ &= \mathbf{d}H(\phi_t(z)) \cdot X_H(\phi_t(z)) \\ &= \Omega_z(X_H(\phi_t(z)), X_H(\phi_t(z))) = 0, \end{aligned}$$

by using the chain rule and bilinearity of Ω in the argument. \square

For the case where the symplectic manifold is also a linear vector space, the pair (\mathcal{M}, Ω) is also referred to as a *symplectic vector space*. We need the following theorems regarding symplectic vector spaces and refer the reader to [18, 30, 11] for detailed proofs.

THEOREM 2. [30] *If (V, Ω) is a symplectic vector space then Ω is a constant form, that is Ω_z is independent of $z \in V$.*

THEOREM 3. [30] *If (V, Ω) is a finite-dimensional symplectic manifold then V is even dimensional.*

THEOREM 4. [18] *(The Symplectic Gram-Schmidt) If (V, Ω) is a $2n$ -dimensional symplectic vector space, then there is a basis $e_1, \dots, e_n, f_1, \dots, f_n$ of V such that*

$$(22) \quad \begin{aligned} \Omega(e_i, e_j) &= 0 = \Omega(f_i, f_j), & i \neq j, \\ \Omega(e_i, f_j) &= \delta_{ij}, & i \leq i, j \leq n. \end{aligned}$$

where δ is the Kronecker's delta function. Moreover, if $V = \mathbb{R}^{2n}$ then we can choose basis vectors $\{e_i, f_i\}_{i=1}^n$ such that

$$(23) \quad \Omega(v_1, v_2) = v_1^T \mathbb{J}_{2n} v_2, \quad v_1, v_2 \in \mathbb{R}^{2n},$$

with \mathbb{J}_{2n} being the standard symplectic matrix, defined as

$$(24) \quad \mathbb{J}_{2n} = \begin{pmatrix} 0_n & I_n \\ -I_n & 0_n \end{pmatrix}.$$

Here I_n and 0_n is the identity matrix and the zero square matrix of size n , respectively.

THEOREM 5. [30] The classical inner product $\langle \cdot, \cdot \rangle : \mathbb{R}^{2n} \times \mathbb{R}^{2n} \rightarrow \mathbb{R}$ can be written in terms of the 2-form as

$$(25) \quad \langle v, u \rangle = \Omega(\mathbb{J}_{2n} v, u), \quad \forall u, v \in \mathbb{R}^{2n}.$$

DEFINITION 6. [18] Suppose (V, Ω) is a finite dimensional symplectic vector space and $E \subset V$ is a subspace. Then the symplectic complement of E inside V is defined as

$$E^\perp := \{v \in V \mid \Omega(v, e) = 0, \forall e \in E\}$$

Note that $E \cap E^\perp$ is not empty in general.

DEFINITION 7. [18] Suppose (V, Ω) is a finite dimensional symplectic vector space. A subspace $E \subset V$ is called a Lagrangian subspace inside V if $E = E^\perp$.

THEOREM 8. [1] Suppose (V, Ω) is a finite dimensional symplectic vector space. If $E \subset V$ is a Lagrangian subspace then $\dim(E) = \frac{1}{2} \dim(V)$. Here \dim denotes the dimension of the subspace.

DEFINITION 9. A basis of (V, Ω) is called orthosymplectic if it is both a symplectic basis and an orthogonal basis with respect to the classical scalar product.

THEOREM 10. [32, 17] Suppose (V, Ω) is a $2n$ dimensional symplectic vector space and $E \subset V$ is a Lagrangian subspace. Then there is an orthosymplectic basis for V .

Proof. We are going to summarize the proof given in [32]. Starting from a Lagrangian subspace in $E \subset V$ an orthosymplectic basis can be easily constructed. By Theorem 8 E is n dimensional. Suppose that $\{e'_1, \dots, e'_n\}$ is a basis for E , using the classical Gram-Schmidt orthogonalization process we can construct an orthonormal basis $\{e_1, \dots, e_n\}$. Define a new set of vectors $f_1 = \mathbb{J}_{2n}^T e_1, f_2 = \mathbb{J}_{2n}^T e_2, \dots, f_n = \mathbb{J}_{2n}^T e_n$. We have

$$(26) \quad \langle f_i, f_j \rangle = e_i^T \mathbb{J}_{2n} \mathbb{J}_{2n}^T e_j = \delta_{ij}, \quad \langle f_i, e_j \rangle = e_i^T \mathbb{J}_{2n} e_j = 0, \quad i, j = 1, \dots, n,$$

where we used the fact that $\mathbb{J}_{2n} \mathbb{J}_{2n}^T = I_{2n}$ in the first identity and the second identity is due to the fact that the basis $\{e_1, \dots, e_n\}$ forms a Lagrangian subspace. This shows that the set $\{e_1, \dots, e_n\} \cup \{f_1, \dots, f_n\}$ forms an orthonormal basis. Also, it can be easily verified that this is a symplectic basis. Thus $\{e_1, \dots, e_n\} \cup \{f_1, \dots, f_n\}$ is an orthosymplectic basis. \square

THEOREM 11. [30] On a finite-dimensional symplectic vector space the relationship (18) becomes

$$(27) \quad \begin{cases} \dot{\mathbf{z}} = \mathbb{J}_{2n} \nabla_{\mathbf{z}} H(\mathbf{z}), \\ \mathbf{z}(0) = \mathbf{z}_0. \end{cases}$$

265 or, by introducing the canonical coordinates $\mathbf{z} = (\mathbf{q}^T, \mathbf{p}^T)^T$,

$$266 \quad (28) \quad \begin{cases} \dot{\mathbf{q}} = \nabla_{\mathbf{p}} H(\mathbf{q}, \mathbf{p}), \\ \dot{\mathbf{p}} = -\nabla_{\mathbf{q}} H(\mathbf{q}, \mathbf{p}). \end{cases}$$

267 Let us now introduce *symplectic transformations*, i.e., mappings between sym-
 268 plectic manifolds which preserve the 2-form Ω . The accurate numerical treatment of
 269 Hamiltonian systems often requires preservation of the symmetry expressed in Theo-
 270 rem 1. Symplectic transformations can be used to construct such symmetry preserving
 271 numerical methods.

272 DEFINITION 12. Let (V, Ω) and (W, Π) be two linear symplectic vector spaces of
 273 dimensions $2n$ and $2k$, respectively. A linear mapping $\phi : V \rightarrow W$ is called symplectic
 274 or canonical if

$$275 \quad (29) \quad \Omega = \phi^* \Pi$$

276 where $\phi^* \Pi$ is the pullback of Π by ϕ , i.e. for all $\mathbf{z}_1, \mathbf{z}_2 \in V$

$$277 \quad (30) \quad \Omega(\mathbf{z}_1, \mathbf{z}_2) = \Pi(\phi(\mathbf{z}_1), \phi(\mathbf{z}_2)).$$

278 Note that if we represent the transformation ϕ as a matrix $A \in \mathbb{R}^{2n \times 2k}$ condition
 279 (29) is equivalent to [30]

$$280 \quad (31) \quad A^T \mathbb{J}_{2n} A = \mathbb{J}_{2k}.$$

281 A matrix of size $2n \times 2k$ satisfying (31) is called a *symplectic matrix*. We emphasize
 282 that a symplectic matrix is conventionally referred to a square matrix, however, here
 283 we may allow symplectic matrices to be also rectangular.

284 DEFINITION 13. The symplectic inverse of a matrix $A \in \mathbb{R}^{2n \times 2k}$ is denoted by
 285 A^+ and defined by [37]

$$286 \quad (32) \quad A^+ := \mathbb{J}_{2k}^T A^T \mathbb{J}_{2n}.$$

287 We point out the properties of the symplectic inverse and refer the reader to [37] for
 288 detailed proof.

289 LEMMA 14. Let $A \in \mathbb{R}^{2n \times 2k}$ be a symplectic matrix and A^+ its symplectic inverse
 290 as defined in (32). Then $(A^+)^T$ is a symplectic matrix and $A^+ A = I_{2k}$.

291 A straight-forward calculation verifies that AA^+ is idempotent, i.e., a symplectic
 292 projection onto the column span of A .

293 It is natural to expect a numerical integrator that solves (27) to also satisfy the
 294 conservation law in Theorem 1. Common numerical integrators e.g., Runge-Kutta
 295 methods, do not generally preserve the Hamiltonian which results in a qualitative
 296 wrong behavior of the solution [20]. Symplectic integrators are a class of numerical
 297 integrators for Hamiltonian systems that preserve the symplectic structure and ensure
 298 stability in long-time integration. The Störmer-Verlet time stepping scheme is an
 299 example of symplectic integrators and is given by

$$300 \quad (33) \quad \begin{aligned} q_{n+1/2} &= q_n + \frac{\Delta t}{2} \nabla_p H(q_{n+1/2}, p_n), \\ p_{n+1} &= p_n - \frac{\Delta t}{2} (\nabla_q H(q_{n+1/2}, p_n) + \nabla_q H(q_{n+1/2}, p_{n+1})), \\ q_{n+1} &= q_{n+1/2} + \frac{\Delta t}{2} \nabla_p H(q_{n+1/2}, p_{n+1}), \end{aligned}$$

301 and

$$\begin{aligned}
 302 \quad (34) \quad p_{n+1/2} &= p_n - \frac{\Delta t}{2} \nabla_q H(q_n, p_{n+1/2}), \\
 q_{n+1} &= q_n + \frac{\Delta t}{2} (\nabla_p H(q_n, p_{n+1/2}) + \nabla_p H(q_{n+1}, p_{n+1/2})), \\
 p_{n+1} &= p_{n+1/2} - \frac{\Delta t}{2} \nabla_q H(q_{n+1}, p_{n+1/2}).
 \end{aligned}$$

303 For a general Hamiltonian system, the Störmer-Verlet scheme is implicit. However, for
 304 separable Hamiltonians, i.e. $H(q, p) = K(p) + U(q)$, this scheme becomes explicit. We
 305 refer the reader to [20] for more information about the construction and applications
 306 of symplectic and geometric numerical integrators.

307 **4. Symplectic Model Reduction.** We now discuss how to modify reduced
 308 order modeling to ensure that the resulting scheme preserves the symplectic structure
 309 of the Hamiltonian system.

310 Consider a Hamiltonian system (27) on a $2n$ -dimensional symplectic vector space
 311 (V, Ω) . Suppose that the solution manifold \mathcal{M}_H is well approximated by a low dimen-
 312 sional symplectic subspace (W, Ω) of dimension $2k$ ($k \ll n$). We can then construct a
 313 symplectic basis A for W and approximate the solution to (27) as

$$314 \quad (35) \quad \mathbf{z} \approx A\mathbf{y}.$$

315 Substituting this into (27) we obtain

$$316 \quad (36) \quad A\mathbf{y} = \mathbb{J}_{2n} \nabla_{\mathbf{z}} H(A\mathbf{y}).$$

317 Multiplying both sides with the symplectic inverse of A and using the chain rule we
 318 have

$$319 \quad (37) \quad \mathbf{y} = A^+ \mathbb{J}_{2n} (A^+)^T \nabla_{\mathbf{y}} H(A\mathbf{y}).$$

320 Since A is a symplectic basis, Lemma 14 ensures that $(A^+)^T$ is a symplectic matrix
 321 i.e., $A^+ \mathbb{J}_{2n} (A^+)^T = \mathbb{J}_{2k}$. By defining the reduced Hamiltonian $\tilde{H} : \mathbb{R}^{2k} \rightarrow \mathbb{R}$ as
 322 $\tilde{H}(\mathbf{y}) = H(A\mathbf{y})$ we obtain the reduced system

$$323 \quad (38) \quad \begin{cases} \frac{d}{dt} \mathbf{y} = \mathbb{J}_{2k} \nabla_{\mathbf{y}} \tilde{H}(\mathbf{y}), \\ \mathbf{y}_0 = A^+ \mathbf{z}_0. \end{cases}$$

324 The system obtained from the Petrov-Galerkin projection in (5) is not a Hamiltonian
 325 system and does not guarantee conservation of the symplectic structure. On the
 326 other hand, we observe that the reduced system in (38) is of the form (27) and,
 327 hence, is a Hamiltonian system, i.e. the symplectic structure will be conserved along
 328 integral curves of (38). Note that the original and the reduced systems are endowed
 329 with different Hamiltonians. In the next proposition we show that the error in the
 330 Hamiltonian is constant in time.

331 **PROPOSITION 15.** *Let $\mathbf{z}(t)$ be the solution of (27) at time t . Further suppose that*
 332 *$\tilde{\mathbf{z}}(t)$ is the approximate solution of the reduced system (38) in the original coordinate*
 333 *system. Then the error in the Hamiltonian defined by*

$$334 \quad (39) \quad \Delta H(t) = |H(\mathbf{z}(t)) - H(\tilde{\mathbf{z}}(t))|,$$

335 *is constant for all $t \in \mathbb{R}$.*

Proof. Let ϕ_t and ψ_t be the Hamiltonian flow of the original and the reduced system respectively. By definition $\mathbf{z}(t) = \phi_t(\mathbf{z}_0)$ and $\mathbf{y}(t) = \psi_t(\mathbf{y}_0)$. Using the definition of the reduced Hamiltonian and Theorem 1 we have

$$(40) \quad H(\tilde{\mathbf{z}}(t)) = H(A\mathbf{y}(t)) = \tilde{H}(\mathbf{y}(t)) = \tilde{H}(\psi_t(\mathbf{y}_0)) = \tilde{H}(\mathbf{y}_0) = \tilde{H}(A^+\mathbf{z}_0) = H(AA^+\mathbf{z}_0).$$

The error in the Hamiltonian can then be written in terms of \mathbf{z}_0 and the symplectic basis A as

$$(41) \quad \Delta H(t) = |H(\mathbf{z}_0) - H(AA^+\mathbf{z}_0)| \quad \square$$

The following theorems provide a strong indication of the stability of the reduced system.

DEFINITION 16. [7] Consider a dynamical system of the form $\dot{\mathbf{z}} = \mathbf{f}(\mathbf{z})$ and suppose that \mathbf{z}_e is an equilibrium point for the system so that $\mathbf{f}(\mathbf{z}_e) = 0$. \mathbf{z}_e is called nonlinearly stable or Lyapunov stable if, for any $\epsilon > 0$, we can find $\delta > 0$ such that for any trajectory ϕ_t , if $\|\phi_0 - \mathbf{z}_e\|_2 \leq \delta$, then for all $0 \leq t < \infty$, we have $\|\phi_t - \mathbf{z}_e\|_2 < \epsilon$, where $\|\cdot\|_2$ is the Euclidean norm.

The following proposition, also known as Dirichlet's theorem [7], states the sufficient condition for an equilibrium point to be Lyapunov stable. We refer the reader to [7] for the proof.

PROPOSITION 17. [7] An equilibrium point \mathbf{z}_e is Lyapunov stable if there exists a scalar function $W : \mathbb{R}^n \rightarrow \mathbb{R}$ such that $\nabla W(\mathbf{z}_e) = 0$, $\nabla^2 W(\mathbf{z}_e)$ is positive definite, and that for any trajectory ϕ_t defined in the neighborhood of \mathbf{z}_e , we have $\frac{d}{dt}W(\phi_t) \leq 0$. Here $\nabla^2 W$ is the Hessian matrix of W .

The scalar function W is referred to as the *Lyapunov function*. In the context of the Hamiltonian systems, a suitable candidate for the Lyapunov function is the Hamiltonian function H . The following theorem shows that when H (or $-H$) is a Lyapunov function, then the equilibrium points of the original and the reduced system are Lyapunov stable [1].

THEOREM 18. Consider a Hamiltonian system of the form (27) together with the reduced system (38). Suppose \mathbf{z}_e is an equilibrium point for (27) and that $\mathbf{y}_e = A^+\mathbf{z}_e$. If H (or $-H$) is a Lyapunov function satisfying Proposition 17, then \mathbf{z}_e and \mathbf{y}_e are Lyapunov stable equilibrium points for (27) and (38), respectively.

Proof. It is a direct consequence of Proposition 17 that \mathbf{z}_e is a local minimum or maximum of (27) and also a Lyapunov stable point. It can be easily checked that if \mathbf{z}_e is a local minimum of H then \mathbf{y}_e is a local minimum for \tilde{H} and an equilibrium point for (38). Also from the chain rule we have

$$(370) \quad \nabla_{\mathbf{y}}^2 \tilde{H} = A^T \nabla_{\mathbf{z}}^2 H A.$$

So for any $\xi \in \mathbb{R}^{2k}$

$$(372) \quad \xi^T \nabla_{\mathbf{y}}^2 \tilde{H} \xi = (A\xi)^T \nabla_{\mathbf{z}}^2 H (A\xi) \geq 0.$$

Here the last inequality is due to the positive definiteness of H . Therefore \tilde{H} is also positive definite. By Proposition 17 we conclude that \mathbf{y}_e is a Lyapunov stable point. \square

While the symplectic structure is not guaranteed to be preserved in the reduced systems obtained by the Petrov-Galerkin projection, the reduced system obtained by the symplectic projection guarantees the preservation of the energy up to the error in the Hamiltonian (39). In the next section we discuss different methods for obtaining a symplectic basis.

4.1. Proper Symplectic Decomposition (PSD). Similar to Section 2.1 we gather snapshots $\mathbf{z}_i = [q_i^T, p_i^T]^T$ in the snapshot matrix S . Suppose that a symplectic basis A of size $2n \times 2k$ and its symplectic inverse A^+ is provided. The Proper Symplectic Decomposition requires that the error of the symplectic projection onto the symplectic subspace be minimized. Hence, the PSD symplectic basis of size $2k$ is the solution to the optimization problem

$$(42) \quad \begin{aligned} & \underset{V \in \mathbb{R}^{2n \times 2k}}{\text{minimize}} && \|S - AA^+S\|_F \\ & \text{subject to} && A^T \mathbb{J}_{2n} A = \mathbb{J}_{2k} \end{aligned}$$

Compared to POD, in (42) the orthogonal projection is replaced with a symplectic projection AA^+ . At first, the minimization looks similar to the one obtained by POD. However, it is well known that symplectic bases are not generally orthogonal, and therefore not norm bounded. This means that numerical errors may become dominant in the symplectic projection [25] which makes the minimization (42) a harder problem than (6).

As the optimization problem (42) is nonlinear, the direct solution is usually expensive. A simplified version of the optimization (42) can be found in [37], but there is no guarantee that the method provides a near optimal basis.

Finding eigen-spaces of Hamiltonian and symplectic matrices is studied in the context of optimal control problems [5, 6, 46, 10] and model reduction of Riccati equations [6], where also an SVD-like decomposition for Hamiltonian and symplectic matrices has been proposed [47]. Specially computation of Lagrangian subspaces of a large scale Hamiltonian matrices using a CS-decomposition is presented in [34, 33]. However, the computation of a large snapshot matrix and use of the mentioned methods to compute its eigen-spaces, is usually computationally demanding. Also, these methods generally do not guarantee the construction of a well-conditioned symplectic basis.

The greedy approach presented in Section 4.1.2 is an iterative method for construction of a symplectic basis. It avoids the evaluation of the full snapshot matrix, hence substantially reduces the computational cost in the offline stage of the symplectic model reduction. Also, by construction, it yields an orthosymplectic basis and therefore a well-conditioned basis.

In Section 4.1.1 we briefly outline non-direct methods for finding solutions to (42), proposed by [37], and assuming a specific structure for A . In Section 4.1.2 we introduce a greedy approach for the symplectic basis generation.

4.1.1. SVD Based Methods for Symplectic Basis Generation.

Cotangent lift. Suppose that A is of the form

$$(43) \quad A = \begin{pmatrix} \Phi & 0 \\ 0 & \Phi \end{pmatrix},$$

where $\Phi \in \mathbb{R}^{n \times k}$ is an orthonormal matrix. It is easy to check that A is a symplectic matrix, i.e., $A^T \mathbb{J}_{2n} A = \mathbb{J}_{2k}$. The construction of A suggests that the range of Φ should cover both the potential and the momentum spaces. Hence, we can construct A by forming the combined snapshot matrix

$$(44) \quad S_{\text{combined}} = [q_1, \dots, q_n, p_1, \dots, p_n], \quad \mathbf{z}_i = (q_i^T, p_i^T)^T,$$

and define $\Phi = [u_1, \dots, u_k]$, where u_i is the i -th left singular vector of S_{combined} . It is shown in [37] that among all symplectic bases of the form (43) cotangent lift minimizes the projection error.

Complex SVD. Suppose instead that A takes the form [37]

$$(45) \quad A = \begin{pmatrix} \Phi & -\Psi \\ \Psi & \Phi \end{pmatrix},$$

while Φ and Ψ are real matrices of size $n \times k$ satisfying conditions

$$(46) \quad \Phi^T \Phi + \Psi^T \Psi = I_k, \quad \Phi^T \Psi = \Psi^T \Phi.$$

It can be checked that A forms a symplectic matrix. To construct A we first define the complex snapshot matrix

$$(47) \quad S_{\text{complex}} = [q_1 + ip_1, \dots, q_N + ip_N].$$

Each left singular vector of S_{complex} now takes the form $u_m = r_m + is_m$. We define

$$(48) \quad \Phi = [r_1, \dots, r_k], \quad \Psi = [s_1, \dots, s_k].$$

One can easily check that (46) is satisfied since the matrix of singular vectors is unitary. It is shown in [37] that among all symplectic bases of the form (45) the complex SVD minimizes the projection error.

4.1.2. The Greedy Approach to Symplectic Basis Generation. Greedy generation of the reduced basis is an iterative procedure which, in each iteration, adds the two best possible basis vectors to the symplectic basis to enhance overall accuracy. In contrast to the cotangent lift and the complex SVD methods, the greedy approach does not require the symplectic basis to have a specific structure. This typically results in a more compact basis and/or more accurate reduced systems. For parametric problems, the greedy approach only requires one numerical solution to be computed per iteration hence saving substantial computational cost in the offline stage.

The orthonormalization step is an essential step in most greedy approaches for basis generation in the context of model reduction [21, 42]. However common orthonormalization processes, e.g. the QR method, destroy the symplectic structure of the original system [10]. Here we use a variation of the QR method known as the SR [45] method which is based on the symplectic Gram-Schmidt method and yields a symplectic basis.

As discussed in Section 3, any finite dimensional symplectic linear vector space has a symplectic basis that satisfies conditions (22). Further, Theorem 10 provides an iterative process for constructing an orthosymplectic basis [31, 45]. To briefly describe the SR method, suppose that an orthosymplectic basis

$$(49) \quad A_{2k} = \{e_1, \dots, e_k\} \cup \{\mathbb{J}_{2n}^T e_1, \dots, \mathbb{J}_{2n}^T e_k\},$$

and a vector $z \notin \text{span}(A_{2k})$ is provided. We aim to symplectically orthogonalize (\mathbb{J}_{2n} -orthogonalize) z with respect to A_{2k} and seek $\alpha_1, \dots, \alpha_k, \beta_1, \dots, \beta_k \in \mathbb{R}$ such that

$$(50) \quad \Omega \left(z + \sum_{i=1}^k \alpha_i e_i + \sum_{i=1}^k \beta_i \mathbb{J}_{2n}^T e_i, \sum_{i=1}^k \bar{\alpha}_i e_i + \sum_{i=1}^k \bar{\beta}_i \mathbb{J}_{2n}^T e_i \right) = 0,$$

for all possible $\bar{\alpha}_1, \dots, \bar{\alpha}_k, \bar{\beta}_1, \dots, \bar{\beta}_k \in \mathbb{R}$. It is easily seen that the unique solution is

$$(51) \quad \alpha_i = -\Omega(z, \mathbb{J}_{2n}^T e_i), \quad \beta_i = \Omega(z, e_i),$$

for $i = 1, \dots, k$. Now define the modified vectors as

$$(52) \quad \tilde{z} = z - \sum_{i=1}^k \Omega(z, \mathbb{J}_{2n}^T e_i) e_i + \sum_{i=1}^k \Omega(z, e_i) \mathbb{J}_{2n}^T e_i.$$

If we introduce $e_{k+1} = \tilde{z}/\|\tilde{z}\|_2$, it is easily checked that e_{k+1} is also orthogonal to A_{2k} with respect to the classical inner product. Therefore $\text{span}\{e_1, \dots, e_{k+1}\}$ forms a Lagrangian subspace and according to Theorem 10 the basis $A_{2k+2} = A_{2k} \cup \{e_{k+1}, \mathbb{J}_{2n}^T e_{k+1}\}$ forms an orthosymplectic basis.

Note that the *SR* method is chosen due to its simplicity and it can be replaced with backward stable routines such as the isotropic Arnoldi or the isotropic Lanczos methods [35].

The key element of the greedy algorithm is the availability of an error function which evaluates the error associated with the model reduction [21]. In the framework of symplectic model reduction, one possible candidate is the error in the Hamiltonian (39). Correctly approximating symplectic systems relies on preservation of the Hamiltonian, hence the error in the Hamiltonian arises as a natural choice. Moreover, since the error in the Hamiltonian depends on the initial condition and the reduced symplectic basis, evaluation of the error does not require the time integration of the full system.

Suppose that a $2k$ -dimensional orthosymplectic basis (49) is generated at the k -th step of the greedy method and we seek to enrich it by two additional vectors. Using the error in the Hamiltonian (41) we search the parameter space to identify the value that maximizes the error in the Hamiltonian

$$(53) \quad \omega_{k+1} := \operatorname{argmax}_{\omega \in \Gamma} \Delta H(\omega).$$

The goal is to approximate the Hamiltonian function as well as possible.

We then propagate (27) in time to produce trajectory snapshots

$$(54) \quad S = \{\mathbf{z}(t_i, \omega_{k+1}) | i = 1, \dots, M\}.$$

The next basis vector is the snapshot that maximises the projection error (42)

$$(55) \quad z := \operatorname{argmax}_{s \in S} \|s - A_{2k} A_{2k}^+ s\|.$$

Finally, we update the basis as

$$(56) \quad e_{k+1} = \tilde{z}, \quad A_{2k+1} = A_{2k} \cup \{e_{k+1}, \mathbb{J}_{2n}^T e_{k+1}\},$$

where \tilde{z} is the vector obtained after applying the symplectic Gram-Schmidt process to z .

Since the maximization over the entire parameter space Γ is impossible, we discretize the parameter set into a grid with N points: $\Gamma_N = \{\omega_1, \dots, \omega_N\}$. However, since the selection of parameters only require the evaluation of the error in the Hamiltonian and not time integration of the original system, then Γ_N can be chosen to be very rich.

We summarize the greedy algorithm for the generation of a symplectic basis in Algorithm 2.

Algorithm 2 The greedy algorithm for generation of a symplectic basis

Input: Tolerated loss in the Hamiltonian δ , parameter set $\Gamma_N = \{\omega_1, \dots, \omega_N\}$, initial condition $\mathbf{z}_0(\omega)$

1. $\omega^* \leftarrow \omega_1$
2. $e_1 \leftarrow \mathbf{z}_0(\omega^*)$
3. $A \leftarrow [e_1, \mathbb{J}_{2n}^T e_1]$
4. $k \leftarrow 1$
5. **while** $\Delta H(\omega) > \delta$ for all $\omega \in \Gamma_N$
6. $\omega^* \leftarrow \operatorname{argmax}_{\omega \in \Gamma_N} \Delta H(\omega)$
7. Compute trajectory snapshots $S = \{\mathbf{z}(t_i, \omega^*) | i = 1, \dots, M\}$
8. $\mathbf{z}^* \leftarrow \operatorname{argmax}_{s \in S} \|s - AA^+ s\|$
9. Apply symplectic Gram-Schmidt on \mathbf{z}^*
10. $e_{k+1} \leftarrow \mathbf{z}^* / \|\mathbf{z}^*\|$
11. $A \leftarrow [e_1, \dots, e_{k+1}, \mathbb{J}_{2n}^T e_1, \dots, \mathbb{J}_{2n}^T e_{k+1}]$
12. $k \leftarrow k + 1$
13. **end while**

Output: Symplectic basis A .

4.1.3. Convergence of the Greedy Method. To show convergence of the greedy method we consider a slightly different version based on the projection error. The error in the Hamiltonian is then introduced as a cheap surrogate to the projection error to accelerate the parameter selection.

Suppose that we are given a compact subset S of \mathbb{R}^{2n} . Our intention is to find a set of vectors $A = \{e_1, \dots, e_k, f_1, \dots, f_k\}$ such that A forms an orthosymplectic basis and any $s \in S$ is well approximated by elements of the subspace $\operatorname{span}(A)$. The modified greedy method for generating basis vectors e_i and f_i is as follows. In the initial step we pick e_1 such that $\|e_1\|_2 = \max_{s \in S} \|s\|_2$. Then define $f_1 = \mathbb{J}_{2n}^T e_1$. It is easy to check that the span of $A_2 = \{e_1, f_1\}$ is orthosymplectic, so A_2 is the first subspace that approximates elements of S . In the k -th step of the greedy method, suppose we have a basis $A_{2k} = \{e_1, \dots, e_k, f_1, \dots, f_k\}$. We define P_{2k} to be a symplectic projection operator that projects elements of S onto $\operatorname{span}(A_{2k})$ and define

$$(57) \quad \sigma_{2k}(s) := \|s - P_{2k}(s)\|_2,$$

as the projection error. Moreover we denote by σ_{2k} the maximum approximation error of S using elements in $\operatorname{span}(A_{2k})$ as

$$(58) \quad \sigma_{2k} := \max_{s \in S} \sigma_{2k}(s).$$

The next set of basis vectors in the greedy selection are

$$(59) \quad e_{k+1} := \operatorname{argmax}_{s \in S} \sigma_{2k}(s), \quad f_{k+1} := \mathbb{J}_{2n}^T e_{k+1}.$$

We emphasize that the sequence of basis vectors generated by the greedy is generally not unique [42, 21].

To estimate the quality of the reduced subspace, it is natural to compare it with the best possible $2k$ -dimensional subspace in the sense of the minimum projection (not necessary symplectic) error. For this we introduce the Kolmogorov n -width [26, 39].

524 DEFINITION 19. Let S be a subset of \mathbb{R}^m and Y_n , $n \leq m$, be a general n -
 525 dimensional subspace of \mathbb{R}^m . The angle between S and Y_n is given by

$$526 \quad (60) \quad E(S, Y_n) := \sup_{s \in S} \inf_{y \in Y_n} \|s - y\|_2.$$

527 The Kolmogorov n -width of S in \mathbb{R}^m is given by

$$528 \quad (61) \quad d_n(S, \mathbb{R}^m) := \inf_{Y_n} E(S, Y_n) = \inf_{Y_n} \sup_{s \in S} \inf_{y \in Y_n} \|s - y\|_2$$

529 For a given subspace Y_n , the angle between S and Y_n measures the worst possible
 530 projection error of elements in S onto Y_n . Hence the Kolmogorov n -width quantifies
 531 how well S can be approximated by an n -dimensional subspace.

532 We seek to show that the decay of σ_{2k} , obtained by the greedy algorithm, has the
 533 same rate as of $d_{2k}(S)$, i.e., the greedy method provides the best possible accuracy
 534 attained by a $2k$ -dimensional subspace.

535 We start by \mathbb{J}_{2n} -orthogonalizing the vectors provided by the greedy algorithm as

$$536 \quad (62) \quad \begin{aligned} \xi_1 &= e_i, & \bar{\xi}_1 &= \mathbb{J}_{2n}^T \xi_1, \\ \xi_i &= e_i - P_{2(i-1)}(e_i), & \bar{\xi}_i &= \mathbb{J}_{2n}^T \xi_i \quad i = 2, 3, \dots \end{aligned}$$

537 The projection of a vector $s \in S$ onto $\text{span}(A_{2k})$ can be written using the symplectic
 538 basis as

$$539 \quad (63) \quad P_{2k}(s) = \sum_{i=1}^k (\alpha_i(s) \xi_i + \bar{\alpha}_i(s) \bar{\xi}_i),$$

540 where $\alpha_i(s)$ and $\bar{\alpha}_i(s)$ for $i = 1, \dots, k$ are the expansion coefficients

$$541 \quad (64) \quad \alpha_i(s) = -\frac{\Omega(\bar{\xi}_i, s)}{\Omega(\xi_i, \bar{\xi}_i)}, \quad \bar{\alpha}_i(s) = \frac{\Omega(\xi_i, s)}{\Omega(\xi_i, \bar{\xi}_i)},$$

542 for any $s \in S$. Since $\bar{\xi}_i$ is \mathbb{J}_{2n} -orthogonal to the $\text{span}(A_{2(k-1)})$ we have

$$543 \quad (65) \quad \begin{aligned} |\alpha_i(s)| &= \frac{|\Omega(\bar{\xi}_i, s)|}{|\Omega(\xi_i, \bar{\xi}_i)|} = \frac{|\Omega(\bar{\xi}_i, s - P_{2(k-1)}(s))|}{|\Omega(\xi_i, \bar{\xi}_i)|} \leq \frac{\|\bar{\xi}_i\|_2 \|s - P_{2(k-1)}(s)\|_2}{\|\xi_i\|_2 \|\bar{\xi}_i\|_2} \\ &= \frac{\|s - P_{2(k-1)}(s)\|_2}{\|e_i - P_{2(k-1)}(e_i)\|_2} \leq 1. \end{aligned}$$

544 Here, we use the fact that $|\Omega(\xi_i, \bar{\xi}_i)| = \|\xi_i\|_2^2 = \|\bar{\xi}_i\|_2^2$ with the last inequality following
 545 from the greedy algorithm which maximizes e_i . Similarly we deduce that $|\bar{\alpha}_i(s)| \leq 1$.

546 We write

$$547 \quad (66) \quad \xi_j = \sum_{i=1}^j (\mu_i^j e_i + \gamma_i^j f_i), \quad \bar{\xi}_j = \sum_{i=1}^j (\lambda_i^j e_i + \eta_i^j f_i), \quad j = 1, 2, \dots$$

548 with

$$549 \quad (67) \quad \begin{aligned} \mu_j^j &= 1, \quad \gamma_j^j = 0, \\ \mu_i^j &= \sum_{l=i}^{j-1} (-\alpha_l(f_j) \mu_i^l + \bar{\alpha}_l(f_j) \gamma_i^l), \quad \gamma_i^j = \sum_{l=i}^{j-1} (-\alpha_l(f_j) \gamma_i^l + \bar{\alpha}_l(f_j) \mu_i^l), \\ \lambda_i^j &= -\gamma_i^j, \quad \eta_i^j = \mu_i^j, \end{aligned}$$

for $j = 2, 3, \dots$. By induction and using the bound in (65) we deduce that

$$(68) \quad \mu_i^j, \gamma_i^j, \lambda_i^j, \eta_i^j \leq 3^{j-i}, \quad \text{for } j \geq i.$$

Now let $2k$ be the dimension of the desired reduced space. Looking at the definition of Kolmogorov n -width we observe that for any $\theta > 1$ we can find a subspace Y_{2k} such that $E(S, Y_{2k}) \leq \theta d_{2k}(S, \mathbb{R}^n)$. Hence we can find vectors $v_1, \dots, v_k, u_1, \dots, u_k \in Y_{2k}$ such that

$$(69) \quad \begin{aligned} \|e_i - v_i\|_2 &\leq \theta d_{2k}(S, \mathbb{R}^n), \\ \|f_i - u_i\|_2 &\leq \theta d_{2k}(S, \mathbb{R}^n). \end{aligned}$$

Now we construct a set of $2(k+1)$ new vectors

$$(70) \quad \zeta_j = \sum_{i=1}^{k+1} \mu_i^j v_i + \gamma_i^j u_i, \quad \bar{\zeta}_j = \sum_{i=1}^{k+1} \lambda_i^j v_i + \eta_i^j u_i.$$

for $j = 1, \dots, k+1$. Note that since u_i and v_i belong to Y_{2k} so does their linear combination including all ζ_j and $\bar{\zeta}_j$. We can use the inequality (68) to write

$$(71) \quad \|\xi_i - \zeta_i\|_2 \leq 3^i \theta d_{2k}(S, \mathbb{R}^n), \quad \|\bar{\xi}_i - \bar{\zeta}_i\|_2 \leq 3^i \theta d_{2k}(S, \mathbb{R}^n).$$

Moreover since Y_{2k} is of dimension $2k$ we find $\kappa_i, i = 1, \dots, 2(k+1)$ such that

$$(72) \quad \sum_{i=1}^{2(k+1)} \kappa_i^2 = 1, \quad \sum_{i=1}^{k+1} \kappa_i \zeta_i + \sum_{i=1}^{k+1} \kappa_{i+k+1} \bar{\zeta}_i = 0.$$

We have

$$(73) \quad \left\| \sum_{i=1}^{k+1} \kappa_i \xi_i + \sum_{i=1}^{k+1} \kappa_{i+k+1} \bar{\xi}_i \right\|_2 = \left\| \sum_{i=1}^{k+1} \kappa_i (\xi_i - \zeta_i) + \sum_{i=1}^{k+1} \kappa_{i+k+1} (\bar{\xi}_i - \bar{\zeta}_i) \right\|_2 \\ \leq 2 \cdot 3^{k+1} \sqrt{2(k+1)} \theta d_{2k}(S, \mathbb{R}^n).$$

We know there exists $1 \leq j \leq 2k+2$ such that $\kappa_j > 1/\sqrt{2(k+1)}$. Without loss of generality let us assume that $j \leq k+1$. This yields

$$(74) \quad \left\| \xi_j + \kappa_j^{-1} \sum_{i=1, i \neq j}^{k+1} \kappa_i \xi_i + \kappa_j^{-1} \sum_{i=1}^{k+1} \kappa_{i+k+1} \bar{\xi}_i \right\|_2 \leq 4 \cdot 3^{k+1} (k+1) \theta d_{2k}(S, \mathbb{R}^n).$$

Define $c = \kappa_j^{-1} \sum_{i=1, i \neq j}^{k+1} \kappa_i \xi_i + \kappa_j^{-1} \sum_{i=1}^{k+1} \kappa_{i+k+1} \bar{\xi}_i$. Using that $\mathbb{J}_{2n}^T c$ is \mathbb{J}_{2n} -orthogonal to ξ_j we recover

$$(75) \quad \begin{aligned} \|\xi_j\|_2 &\leq \|\xi_j\|_2 + \|c\|_2 = \Omega(\xi_j, \mathbb{J}_{2n}^T \xi_j) + \Omega(c, \mathbb{J}_{2n}^T c) \\ &= \Omega(\xi_j, \mathbb{J}_{2n}^T \xi_j) + \Omega(c, \mathbb{J}_{2n}^T c) + \Omega(\xi_j, \mathbb{J}_{2n}^T c) + \Omega(c, \mathbb{J}_{2n}^T \xi_j) \\ &= \Omega(\xi_j + c, \mathbb{J}_{2n}^T (\xi_j + c)) = \|\xi_j + c\|_2 \end{aligned}$$

Combining this with (74) yields

$$(76) \quad \|\xi_j\|_2 \leq 4 \cdot 3^{k+1} (k+1) \theta d_{2k}(S, \mathbb{R}^n).$$

Finally using the definition of ξ_j for all $s \in S$ we have

$$(77) \quad \|s - P_{2(j-1)}(s)\|_2 \leq \|f_j - P_{2(j-1)}(f_j)\|_2 = \|\xi_j\|_2 \leq 4 \cdot 3^{k+1}(k+1)\theta d_{2k}(S, \mathbb{R}^n)$$

Hence, for any given $\lambda > 1$

$$(78) \quad \|s - P_{2k}(s)\|_2 \leq \|s - P_{2(j-1)}(s)\|_2 \leq 4 \cdot 3^{k+1}(k+1)\theta d_{2k}(S, \mathbb{R}^n).$$

This establishes the following theorem.

THEOREM 20. *Let S be a compact subset of \mathbb{R}^{2n} with exponentially small Kolmogorov n -width $d_k \leq c \exp(-\alpha k)$ with $\alpha > \log 3$. Then there exists $\beta > 0$ such that the symplectic subspaces A_{2k} generated by the greedy algorithm provide exponential approximation properties such that*

$$(79) \quad \|s - P_{2k}(s)\|_2 \leq C \exp(-\beta k)$$

for all $s \in S$ and some $C > 0$.

4.2. Symplectic Discrete Empirical Interpolation Method (SDEIM).

Consider the Hamiltonian system (27) and its reduced system (38) equipped with a symplectic transformation A . One can split the Hamiltonian function $H = H_1 + H_2$ such that $\nabla H_1 = L\mathbf{z}$ and $\nabla H_2 = \mathbf{g}(\mathbf{z})$, where L is a constant matrix in $\mathbb{R}^{2n \times 2n}$ and \mathbf{g} is a nonlinear function. The reduced system takes the form

$$(80) \quad \frac{d}{dt}\mathbf{y} = \underbrace{A^+ \mathbb{J}_{2n} L A}_{\tilde{L}} \mathbf{y} + A^+ \mathbb{J}_{2n} \mathbf{g}(A\mathbf{y})$$

As discussed in Section 2.2, the complexity of evaluating the nonlinear term still depends on n , the size of the original system. To overcome this computational bottleneck we use the DEIM approximation for evaluating the nonlinear function \mathbf{g} as

$$(81) \quad \frac{d}{dt}\mathbf{y} = \tilde{L}\mathbf{y} + \underbrace{A^+ \mathbb{J}_{2n} V (P^T V)^{-1} P^T \mathbf{g}(A\mathbf{y})}_{\tilde{N}(\mathbf{y})}$$

For a general choice of V the system (81) is not guaranteed to be a Hamiltonian system, impacting long time accuracy and stability. However, we can guarantee that (81) is a Hamiltonian system by choosing $V = (A^+)^T$. To see this, we note that the system (81) is a Hamiltonian system if and only if $\tilde{N}(\mathbf{y}) = \mathbb{J}_{2k} \nabla_{\mathbf{y}} \mathbf{g}(\mathbf{y})$. Also we have

$$(82) \quad \mathbf{g}(A\mathbf{y}) = \nabla_{\mathbf{z}} H_2(\mathbf{z}) = (A^+)^T \nabla_{\mathbf{y}} H_2(A\mathbf{y}),$$

where the chain rule is used for the second equality. Substituting this into \tilde{N} we obtain

$$(83) \quad \tilde{N}(\mathbf{y}) = A^+ \mathbb{J}_{2n} V (P^T V)^{-1} P^T (A^+)^T \nabla_{\mathbf{y}} H_2(A\mathbf{y}).$$

Taking $V = (A^+)^T$ yields

$$(84) \quad \tilde{N}(\mathbf{y}) = A^+ \mathbb{J}_{2n} (A^+)^T \nabla_{\mathbf{y}} H_2(A\mathbf{y}) = \mathbb{J}_{2k} \nabla_{\mathbf{y}} H_2(A\mathbf{y}),$$

since $(A^+)^T$ is a symplectic matrix. Hence, $V = (A^+)^T$ is a sufficient condition for (81) to be Hamiltonian.

Regarding the construction of the projection space, suppose that we have already constructed a symplectic basis $A = \{e_1, \dots, e_k, f_1, \dots, f_k\}$ using the greedy algorithm. Note that $(A^+)^T$ is a symplectic basis and $(A^+)^+ = A$. Thus, we can move between these two symplectic bases by simply using the transpose operator and the symplectic inverse operator. Let $S_{\mathbf{g}} = \{\mathbf{g}(\mathbf{x}(t_i, \omega_j))\}$ with $i = 1, \dots, M$ and $j = 1, \dots, N$ be the nonlinear snapshots that were gathered in the greedy algorithm. We then form $(A^+)^T = \{e'_1, \dots, e'_k, f'_1, \dots, f'_k\}$ and use a greedy approach to add new basis vectors to $(A^+)^T$. At the i -th iteration of the symplectic DEIM, we use $(A^+)^T$ to approximate elements in $S_{\mathbf{g}}$ and choose the vector that maximizes the error as the next basis vector

$$(85) \quad s^* := \operatorname{argmax}_{s \in S_{\mathbf{g}}} \|s - (A^+)^T A^+ s\|_2.$$

After applying the symplectic Gram-Schmidt on s^* , we update $(A^+)^T$ as

$$(86) \quad e'_{k+i+1} = \frac{s^*}{\|s^*\|_2}, \quad f'_{k+i+1} = \mathbb{J}_{2n}^T e'_{k+i+1}.$$

Finally when $(A^+)^T$ approximates elements $S_{\mathbf{g}}$ with the desired accuracy, we transpose and symplectically invert $(A^+)^T$ to obtain A . We summarize the symplectic DEIM algorithm in Algorithm 3.

Algorithm 3 Symplectic Discrete Empirical Interpolation Method

Input: Symplectic basis $A = \{e_1, \dots, e_k, f_1, \dots, f_k\}$, nonlinear snapshots $S_{\mathbf{g}} = \{\mathbf{g}(\mathbf{x}(t_i, \omega_j))\}$ and tolerance δ

1. Compute $(A^+)^T = \{e'_1, \dots, e'_k, f'_1, \dots, f'_k\}$
2. $i \leftarrow 1$
3. **while** $\max_{s \in S_{\mathbf{g}}} \|s - (A^+)^T A^+ s\| > \delta$ **for all** $s \in S_{\mathbf{g}}$
4. $s^* \leftarrow \operatorname{argmax}_{s \in S_{\mathbf{g}}} \|s - (A^+)^T A^+ s\|$
5. Apply symplectic Gram-Schmidt on s^*
6. $e'_{k+i} = s^* / \|s^*\|$
7. $f'_{k+i} = \mathbb{J}_{2n} e'_{k+i}$
8. $(A^+)^T \leftarrow [e'_1, \dots, e'_{k+i}, f'_1, \dots, f'_{k+i}]$
9. $i \leftarrow i + 1$
10. **end while**
11. take transpose and symplectic inverse of $(A^+)^T$

Output: Symplectic basis A that guarantees a Hamiltonian reduced system.

When using an implicit time integration scheme we face inefficiencies when evaluating the Jacobian of nonlinear terms, as discussed in Section 2.2. We recall that the key to fast approximation of the Jacobian is that the interpolating index matrix P , obtained in the DEIM approximation, commutes with the nonlinear function. Nonlinear terms in Hamiltonian systems often take the form

$$(87) \quad \mathbf{g}(\mathbf{z}) = \mathbf{g}(\mathbf{q}, \mathbf{p}) = \begin{pmatrix} g_1(q_1, p_1) \\ g_2(q_2, p_2) \\ \vdots \\ g_{2n}(q_n, p_n) \end{pmatrix}.$$

Thus, the interpolating index matrix, obtained by Algorithm 1 does not necessarily commute with the function \mathbf{g} . To overcome this, when index \mathbf{p}_i with $\mathbf{p}_i \leq n$ or $\mathbf{p}_i > n$ is chosen in Algorithm 1 we also include $\mathbf{p}_i + n$ or $\mathbf{p}_i - n$, respectively. Simple calculations verifies that \mathbf{g} and P then commute.

In case \mathbf{g} is not of the form (87) one can use MDEIM [13, 36] to accelerate the assembling of the Jacobian matrix.

5. Numerical Results. In this section, we illustrate the performance of the greedy generation of a symplectic basis. The parametric linear wave equation is considered to compare SVD based methods with the greedy method. The symplectic model reduction of nonlinear systems is then illustrated by considering the parametric nonlinear Schrödinger equation. Finally we discuss the numerical convergence of the greedy method introduced in Algorithm 2.

5.1. Parametric Linear Wave equation. Consider the parametric linear wave equation

$$(88) \quad \begin{cases} u_{tt}(x, t, \omega) = \kappa(\omega)u_{xx}(x, t, \omega), \\ u(x, 0) = u^0(x), \end{cases}$$

where x belongs to a one-dimensional torus of length L , $\omega = (\omega_1, \dots, \omega_4)$ and

$$(89) \quad \kappa(\omega) = c^2 \left(\sum_{l=1}^4 \frac{1}{l^2} \omega_l \right).$$

Here $\omega_l \in [0, 1]$ for $l = 1, \dots, 4$ and $c \in \mathbb{R}$ is a constant number. By rewriting (88) in canonical form, using the change of variable $q = u$ and $\partial q / \partial t = p$, we obtain the symplectic form

$$(90) \quad \begin{cases} q_t(x, t, \omega) = p(x, t, \omega), \\ p_t(x, t, \omega) = \kappa(\omega)q_{xx}(x, t, \omega), \end{cases}$$

with the associated Hamiltonian

$$(91) \quad H(q, p, \omega) = \frac{1}{2} \int_0^L p^2 + \kappa(\omega)q_x^2 \, dx.$$

We discretize the torus into N equidistant points and define $\Delta x = L/N$, $x_i = i\Delta x$, $q_i = q(t, x_i, \omega)$ and $p_i = p(t, x_i, \omega)$ for $i = 1, \dots, N$. Furthermore, we discretize (90) using a standard central finite differences scheme to obtain

$$(92) \quad \frac{d}{dt} \mathbf{z} = \mathbb{J}_{2N} L \mathbf{z},$$

where $\mathbf{z} = (q, \dots, q_N, p_q, \dots, p_n)^T$ and

$$(93) \quad L = \begin{pmatrix} I_n & 0_N \\ 0_N & \kappa(\omega) D_{xx} \end{pmatrix},$$

with D_{xx} the central finite differences matrix operator. The discrete Hamiltonian can finally be written as

$$(94) \quad H_{\Delta x}(\mathbf{z}) = \frac{\Delta x}{2} \sum_{i=1}^N \left(p_i^2 + \kappa(\omega) \frac{(q_{i+1} - q_i)^2}{2\Delta x^2} + \kappa(\omega) \frac{(q_i - q_{i-1})^2}{2\Delta x^2} \right).$$

660 The initial condition is given by

$$661 \quad (95) \quad q_i(0) = h(10 \times |x_i - \frac{1}{2}|), \quad p_i = 0, \quad i = 1, \dots, N$$

662 where $h(s)$ is the cubic spline function

$$663 \quad (96) \quad h(s) = \begin{cases} 1 - \frac{3}{2}s^2 + \frac{3}{4}s^3, & 0 \leq s \leq 1, \\ \frac{1}{4}(2-s)^3, & 1 < s \leq 2, \\ 0, & s > 2. \end{cases}$$

664 This will result in waves propagating in both directions on the torus.

665 For numerical time integration we use the Störmer-Verlet (33) scheme, which is
666 explicit since the Hamiltonian is separable for the linear wave-equation. The full
667 model uses the following parameter set

Domain length	$L = 1$
No. grid points	$N = 500$
Space discretization size	$\Delta x = 0.002$
Time discretization size	$\Delta t = 0.01$
Wave speed	$c^2 = 0.1$

669 We compare the reduced system obtained by the greedy algorithm with the methods
670 based on SVD. To generate snapshots, we discretize the parameter space $[0, 1]^4$ into in
671 total of 5^4 equidistant grid points. For the SVD based methods and POD, snapshots
672 are gathered in the snapshot matrices S , S_{combined} and S_{complex} , respectively, and
673 the SVD is performed to construct the reduced basis. The greedy method is applied
674 following Algorithm 2; as input, the tolerance for the error in the Hamiltonian is set
675 to $\delta = 5 \times 10^{-3}$. All reduced systems are taken to have an identical size ($k = 80$ for
676 POD and $k = 40$ for the symplectic methods). We use the Störmer-Verlet scheme
677 for symplectic methods and a second order Runge-Kutta method for the POD. The
678 choice of different time integration routines is due to the fact that the POD destroys
679 the canonical form of the original equations and a symplectic integrator cannot be
680 applied. One can alternatively use separate reduced subspaces for the potential and
681 the momentum spaces, which however is not a standard model reduction approach and
682 requires further analysis. Finally we use transformation (35) to transfer the solution
683 of the reduced systems into the high-dimensional space for illustration purposes.

684 We reduced the cost by 50% in the offline stage when using the greedy method
685 as compared to SVD-based methods (cotangent lift and complex SVD method). This
686 happens because the SVD-based methods require time integration of the full system
687 for all discrete parameter points, while the greedy method picks a number of param-
688 eters from the parameter space.

689 Figure 1a shows the solution of the linear wave equation for parameter values
690 $(\omega_1, \omega_2, \omega_3, \omega_4) = (0.8456, 0.1320, 0.9328, 0.5809)$ or $\kappa(\omega) = 0.1019$, chosen to be dif-
691 ferent from training parameters, at $t = 0$, $t = 1$ and $t = 2$. While we see instability
692 and divergence from the exact solution for the POD reduced system, the symplectic
693 methods provide a good approximation of the full model.

694 The decay of the singular values for the POD are shown in Figure 5a. The decay
695 of the singular values suggests that a low dimensional solution manifold indeed exists.

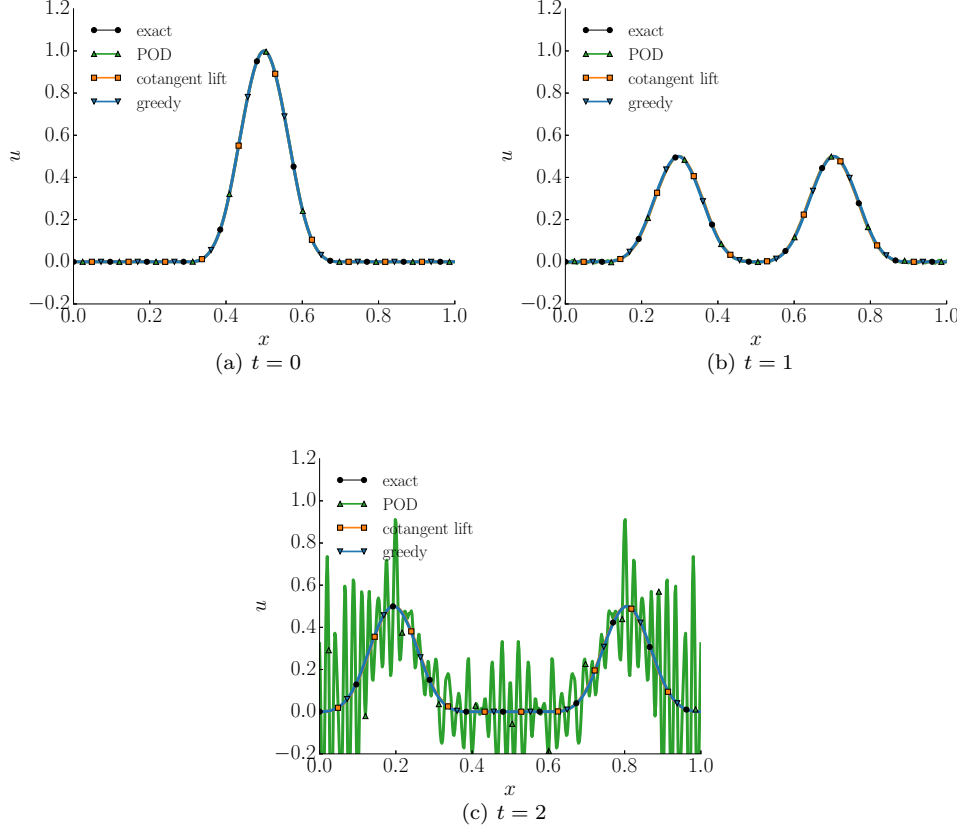


Fig. 1: The solution q at $t = 0$, $t = 1$ and $t = 2$ of the linear wave equation for parameter value $c = 0.1019$ different from training parameters. Here, the solution of the full system together with the solution of the POD, cotangent lift, complex SVD and the greedy reduced system is shown.

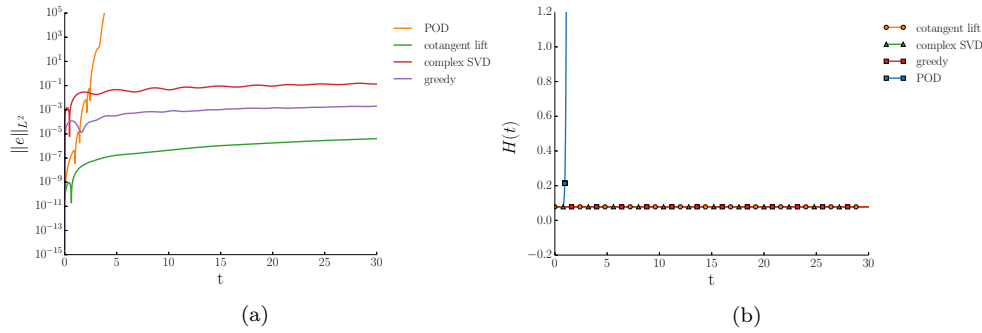


Fig. 2: (a) The L^2 -error between the solution of the full system and the reduced system for different model reduction methods for $t \in [0, 30]$. (b) Plot of the Hamiltonian function for $t \in [0, 30]$.

However, since the linear subspace, constructed by the POD, is not symplectic, we observe blow up of the Hamiltonian function in Figure 2b and the instability of the solution in Figure 1. The symplectic methods (using a reduced basis of the same size as POD) preserve the Hamiltonian function as shown in Figure 2b.

Figure 2a shows the L^2 -error between the solution of the full model and the reduced systems constructed by different methods. We note that the error for the POD reduced system rapidly increases, confirming that the projection based reduced system does not yield a stable solution. Furthermore, the symplectic methods provide a better approximation since the geometric structure of the original system is preserved. Although the greedy method is almost twice faster than the SVD-based methods in the offline stage, its accuracy is comparable. The cotangent lift method provides a more accurate solution, on the other hand the cotangent lift basis (43) takes a less general form and usually computationally more demanding than the greedy method.

For complex systems were the solution of the full system is expensive and for high dimensional parameter domains, POD-based methods become impractical [21, 42]. However, the greedy method requires substantially fewer (proportional to the size of the reduced basis) evaluation of the time integration of the original system.

5.2. Nonlinear Schrödinger equation. Let us consider the one-dimensional parametric Schrödinger equation

$$(97) \quad \begin{cases} iu_t(t, x, \epsilon) = -u_{xx}(t, x, \epsilon) - \epsilon|u(t, x, \epsilon)|^2 u(t, x, \epsilon), \\ u(0, x) = u_0(x), \end{cases}$$

where u is a complex valued wave function, i is the imaginary unit, $|\cdot|$ is the modulus operator and ϵ is a parameter that belongs to the interval $\Gamma = [0.9, 1.1]$. We consider periodic boundary conditions, i.e., x belongs to a one-dimensional torus of length L . We consider the initial condition

$$(98) \quad u_0(x) = \frac{\sqrt{2}}{\cosh(x - x_0)} \exp(i \frac{c(x - x_0)}{2}),$$

for a positive constant c . In quantum mechanics, the quantity $|u(t, x)|^2$ represents the probability of finding the system in state x at time t . For the choice of $\epsilon = 1$, $|u(x, t)|$ becomes a solitary wave, and the initial condition will be transported in the positive x direction with a constant speed. For other choices of ϵ , the solution comprises an ensemble of solitary waves, moving in either direction [19].

By introducing the real and imaginary variables $u = p + iq$, we can rewrite (97) in canonical form as

$$(99) \quad \begin{cases} q_t = p_{xx} + \epsilon(q^2 + p^2)p, \\ p_t = -q_{xx} - \epsilon(q^2 + p^2)q, \end{cases}$$

with the Hamiltonian function

$$(100) \quad H(q, p) = \int_0^L (q_x^2 + p_x^2) + \frac{\epsilon}{2}(q^2 + p^2)^2 dx.$$

We discretize the torus into N equidistant points and take $\Delta x = L/N$, $x_i = i\Delta x$, $q_i = q(t, x_i, \epsilon)$ and $p_i = p(t, x_i, \omega)$ for $i = 1, \dots, N$. A central finite differences scheme is used to discretize (99) as

$$(101) \quad \frac{d}{dt} \mathbf{z} = \mathbb{J}_{2N} L \mathbf{z} + \mathbb{J}_{2N} \mathbf{g}(\mathbf{z}).$$

735 Here $\mathbf{z} = (q_1, \dots, q_N, p_1, \dots, p_N)^T$ and

736 (102)
$$L = \begin{pmatrix} D_{xx} & 0_N \\ 0_N & D_{xx} \end{pmatrix}.$$

737 Here \mathbf{g} is a vector valued nonlinear function defined as

738 (103)
$$\mathbf{g}(\mathbf{z}) = \begin{pmatrix} (q_1^2 + p_1^2)q_1 \\ \vdots \\ (q_N^2 + p_N^2)q_N \\ (q_1^2 + p_1^2)p_1 \\ \vdots \\ (q_N^2 + p_N^2)p_N \end{pmatrix}.$$

739 We discretize the Hamiltonian to obtain

740 (104)
$$H_{\Delta x}(\mathbf{z}) = \Delta x \sum_{i=1}^N \left(\frac{q_i q_{i-1} - q_i^2}{\Delta x^2} + \frac{p_i p_{i-1} - p_i^2}{\Delta x^2} + \frac{\epsilon}{4} (p_i^2 + q_i^2)^2 \right),$$

741 and use a Störmer-Verlet (33) scheme for time integration. Since the Hamiltonian
 742 function (104) is non-separable, this scheme becomes implicit so in each time iteration,
 743 a system of nonlinear equations is solved using Newton's iteration. We summarize
 744 the physical and numerical parameters for the full model in the following table

745

Domain length	$L = 2\pi/l$
Domain scaling factor	$l = 0.11$
wave speed	$c = 1$
No. grid points	$N = 256$
Space discretization size	$\Delta x = 0.2231$
Time discretization size	$\Delta t = 0.01$

746 Regarding computation of the nonlinear terms of reduced systems, we compare the
 747 DEIM with the symplectic DEIM. For generation of the DEIM reduced basis we apply
 748 Algorithm 1 to the set of nonlinear snapshots. Algorithm 3 is used to construct a re-
 749 duced basis appropriate for the symplectic DEIM. As input, we provide the symplectic
 750 basis generated by Algorithm 2 with the set of nonlinear snapshots and a tolerance
 751 for the error $\delta = 10^{-4}$.

752 We compare the reduced system obtained using the greedy algorithm with the
 753 cotangent lift, the complex SVD, DEIM, the symplectic DEIM and also the POD. For
 754 the SVD-based methods, we discretize the parameter space $[0.9, 1.1]$ into $M = 500$
 755 equidistant grid points across the discrete parameter space $\Gamma_M = \{\epsilon_1, \dots, \epsilon_M\}$, and
 756 gather trajectory snapshots for each ϵ_i for $i = 1, \dots, M$ in the snapshots matrix S . All
 757 reduced systems are taken to have identical sizes ($k = 90$ for the symplectic methods
 758 and $k = 180$ for the POD method). Following Algorithm 2 we construct the reduced
 759 system using the same discrete parameter space Γ_M . The tolerance for the error in
 760 the Hamiltonian is set to $\delta = 10^{-3}$. Moreover, for DEIM and symplectic DEIM,
 761 we construct bases of size $k' = 80$. Note that the reduced system, generated in the
 762 symplectic DEIM, will be of size $k + k' = 170$.

763 The cost of the offline stage is reduced to 20% when using the greedy method
 764 for constructing a symplectic basis of size $k = 90$, as compared to the SVD-based

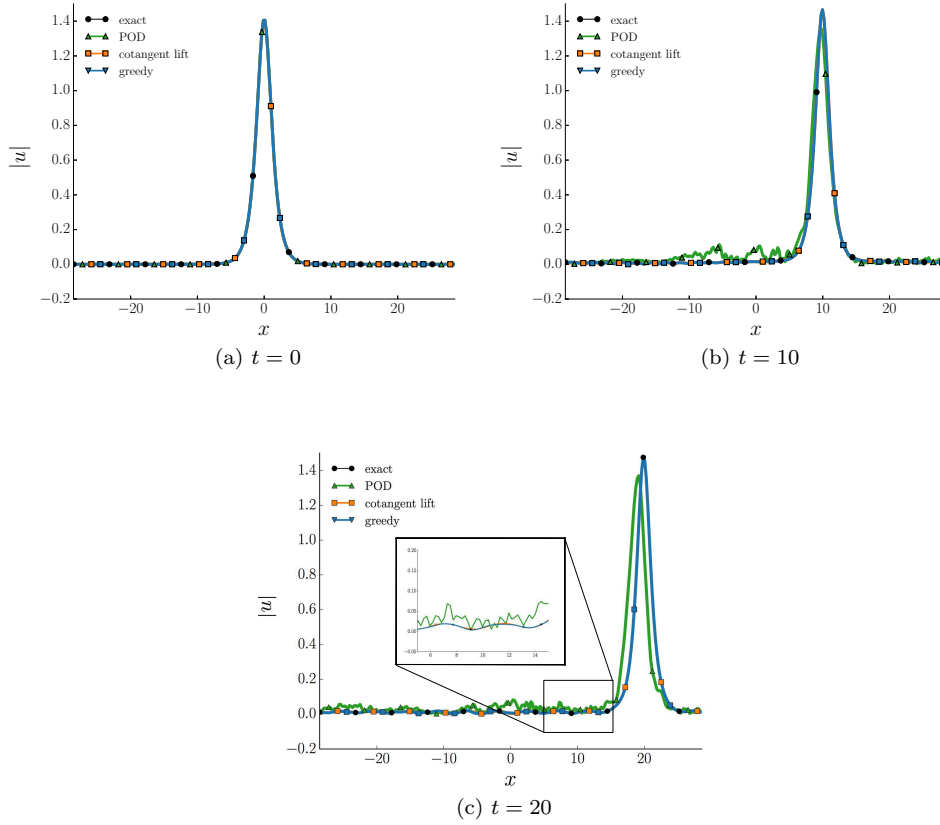


Fig. 3: The solution $|u(t, x)| = \sqrt{q^2 + p^2}$ at $t = 0$, $t = 10$ and $t = 20$ of the Nonlinear Schrödinger equation for parameter value $\epsilon = 1.0932$. Here the solution of the full system, together with the solution of the POD, cotangent lift, complex SVD and the greedy reduced system, is shown.

methods. The online stage, i.e., time integration for a new parameter in Γ , is generally more than 3 times faster than for the original system. We point out that the efficiency of reduced systems are implementation and platform dependent and we expect further reduction as the size of the problem increases.

Figure 3 shows the solution of the Schrödinger equation for parameter value $\epsilon = 1.0932$ at $t = 0$, $t = 10$ and $t = 20$. We first compare the reduced system obtained by the greedy algorithm with the POD, the cotangent lift, and the complex SVD method. The size of the reduced systems are taken identical for all methods ($k = 180$ for POD and $k = 90$ for the rest). Although the decay of the singular values in Figure 5b suggests that the accuracy of the POD reduced system should be comparable to that of the other methods, we observe instabilities in the solution at $t = 10$. The greedy, the cotangent lift and the complex SVD method, on the other hand, generate a stable reduced system that accurately approximates the solution of the full model.

In Figure 4b we observe that the symplectic methods preserve the Hamiltonian function, unlike the POD and the DEIM methods. We emphasise that using the

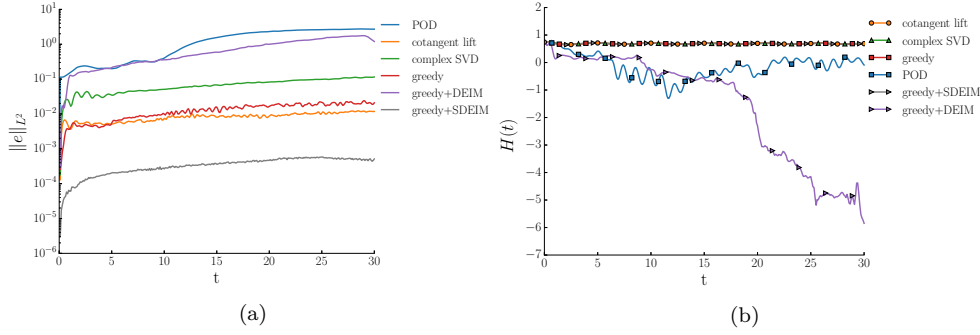


Fig. 4: (a) Plot of the Hamiltonian function for $t \in [0, 30]$. (b) The L^2 error between the solution of the full system and the reduced system for different model reduction methods for $t \in [0, 30]$.

reduced basis, obtained by the greedy, together with the DEIM (purple line) does not preserve the symplectic structure as suggested in this figure.

Figure 4a illustrates the L^2 -error between the solution of the full model with the reduced systems, generated by different methods. We first observe that symplectic methods yield a lower computational error when compared to non-symplectic methods. Secondly, we observe that although the reduced systems from the cotangent lift and the complex SVD are of the same size, their accuracy is different by an order of magnitude. We notice that the greedy algorithm is slightly less accurate than the cotangent lift method while its offline computational cost is reduced to 20% when compared to the cotangent lift. Lastly we notice that the combination of the greedy reduced basis and DEIM yields large errors in the solution while the solution using the symplectic DEIM is very accurate. We note that the symplectic DEIM is even more accurate than the greedy itself since it has been enriched by the nonlinear snapshots.

5.3. Numerical Convergence. In this section we discuss the numerical convergence of the symplectic greedy method introduced in Section 4. The exponential convergence properties of the conventional greedy [42] is presented in [9, 8]. Theorem 20 suggests that the symplectic greedy method has similar properties. To illustrate this we compare the convergence of the conventional greedy with the convergence of the symplectic greedy method through the numerical simulations in Sections 5.1 and 5.2.

The decay of the singular values of the snapshot matrix for the parametric wave equation and the nonlinear Schrödinger equation are given in Figure 5. The decay rate of the singular values is a strong indicator for the decay rate of the Kolmogorov n -width of the solution manifold. We expect that the conventional greedy method and the symplectic greedy method provide a similar rate in the decay of the error.

Figure 5 shows the maximum L^2 error between the original system and the reduced system at each iteration of different greedy methods. In this figure we find the conventional greedy with orthogonal projection error as a basis selection criterion (orange), the symplectic greedy method with a symplectic projection error as a basis selection criterion (green), and the symplectic greedy method with energy loss ΔH as a basis selection criterion (red).

It is observed that the decay rate of the error for greedy with the orthogonal

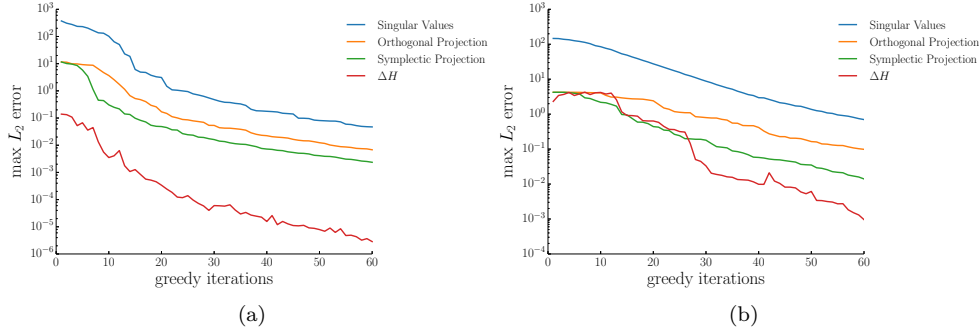


Fig. 5: (a) Convergence of the greedy method for the wave equation. (b) Convergence of the greedy method for the nonlinear Schrödinger equation equation.

projection and the greedy with the symplectic projection is similar to the decay of the singular values. This matches our expectation from Theorem 20. We also notice that the greedy method with the loss in Hamiltonian provides an excellent error indication as a basis selection criterion.

6. Conclusion. In this paper, we present a greedy approach for the construction of a reduced system that preserves the geometric structure of Hamiltonian systems. An iteration of the greedy method comprises searching the parameter space using the error in the Hamiltonian, to find the best basis vectors that increase the overall accuracy of the reduced basis. We argue that for a compact subset with exponentially small Kolmogorov n -width we recover exponentially fast convergence of the greedy algorithm. For fast approximation of nonlinear terms, the basis obtained by the greedy was combined with a symplectic DEIM to construct a reduced system with a Hamiltonian that is arbitrary close to the Hamiltonian of the original system.

The numerical results demonstrate that the greedy method can save substantial computational cost in the offline stage as compared to alternative SVD-based techniques. Also since the reduced system obtained by the greedy method is Hamiltonian, the greedy method yields a stable reduced system. Symplectic DEIM effectively reduces computational cost of approximating nonlinear terms while preserving stability and symplectic structure. Hence, the greedy method is an efficient model reduction technique that provides an accurate and stable reduced system for large-scale parametric Hamiltonian systems.

Acknowledgments. We would like to thank the referees for providing us with very useful comments which served to improve the paper.

REFERENCES

- [1] R. ABRAHAM AND J. MARSDEN, *Foundations of Mechanics*, AMS Chelsea publishing, AMS Chelsea Pub./American Mathematical Society, 1978, <https://books.google.ch/books?id=YAEBBAAQBAJ>.
- [2] A. C. ANTOUNAS, *Approximation of Large-Scale Dynamical Systems*, SIAM, June 2009.
- [3] J. A. ATWELL AND B. B. KING, *Proper orthogonal decomposition for reduced basis feedback controllers for parabolic equations*, Mathematical and Computer Modelling, 33 (2001), pp. 1–19.

- [4] M. BARRAULT, Y. MADAY, N. C. NGUYEN, AND A. T. PATERA, *An ‘empirical interpolation’ method: application to efficient reduced-basis discretization of partial differential equations*, *Comptes Rendus Mathématique*, 339 (2004), pp. 667–672.
- [5] P. BENNER, R. BYERS, H. FASSBENDER, V. MEHRMANN, AND D. WATKINS, *Cholesky-like factorizations of skew-symmetric matrices*, *Electronic Transactions on Numerical Analysis*, 11 (2000), pp. 85–93 (electronic).
- [6] P. BENNER, V. MEHRMANN, AND H. XU, *A new method for computing the stable invariant subspace of a real Hamiltonian matrix*, *Journal of Computational and Applied Mathematics*, 86 (1997), pp. 17–43.
- [7] N. BHATIA AND G. SZEGÖ, *Stability Theory of Dynamical Systems*, *Classics in Mathematics*, Springer Berlin Heidelberg, 2002, <https://books.google.ch/books?id=wP5dwTS6jg0C>.
- [8] P. BINEV, A. COHEN, W. DAHMEN, R. DEVORE, G. PETROVA, AND P. WOJTASZCZYK, *Convergence rates for greedy algorithms in reduced basis methods*, *SIAM Journal on Mathematical Analysis*, 43 (2011), pp. 1457–1472.
- [9] A. BUFFA, Y. MADAY, A. T. PATERA, C. PRUD’HOMME, AND G. TURINICI, *A priori convergence of the greedy algorithm for the parametrized reduced basis method*, *ESAIM. Mathematical Modelling and Numerical Analysis*, 46 (2012), pp. 595–603.
- [10] A. BUNSE-GERSTNER, *Matrix factorizations for symplectic QR-like methods*, *Linear Algebra and its Applications*, 83 (1986), pp. 49–77.
- [11] A. CANNAS DA SILVA, *Lectures on symplectic geometry*, vol. 1764 of *Lecture Notes in Mathematics*, Springer-Verlag, Berlin, Berlin, Heidelberg, 2001.
- [12] K. CARLBERG, R. TUMINARO, AND P. BOGGS, *Preserving Lagrangian structure in nonlinear model reduction with application to structural dynamics*, *SIAM Journal on Scientific Computing*, (2015).
- [13] K. CARLBERG, R. TUMINARO, AND P. BOGGSZ, *Efficient structure-preserving model reduction for nonlinear mechanical systems with application to structural dynamics*, preprint, Sandia National Laboratories, Livermore, CA, 94551 (2012).
- [14] S. CHATURANTABUT, C. BEATTIE, AND S. GUGERCIN, *Structure-Preserving Model Reduction for Nonlinear Port-Hamiltonian Systems*, *SIAM Journal on Scientific Computing*, 38 (2016), pp. B837–B865.
- [15] S. CHATURANTABUT AND D. C. SORENSEN, *Nonlinear Model Reduction via Discrete Empirical Interpolation*, *SIAM Journal on Scientific Computing*, 32 (2010), pp. 2737–2764.
- [16] N. N. CUONG, K. VERVOY, AND A. T. PATERA, *Certified Real-Time Solution of Parametrized Partial Differential Equations*, in *Handbook of Materials Modeling*, Springer Netherlands, Dordrecht, 2005, pp. 1529–1564.
- [17] A. DA SILVA, *Introduction to Symplectic and Hamiltonian Geometry*, *Publicações matemáticas*, IMPA, 2003, https://books.google.ch/books?id=_X8QAgAACAAJ.
- [18] M. DE GOSSON, *Symplectic Geometry and Quantum Mechanics*, *Operator Theory: Advances and Applications*, Birkhäuser Basel, 2006, <https://books.google.ch/books?id=q9SHRvay75IC>.
- [19] E. FAOU, *Geometric Numerical Integration and Schrödinger Equations*, *European Mathematical Society*, 2012.
- [20] E. HAIRER, C. LUBICH, AND G. WANNER, *Geometric Numerical Integration: Structure-Preserving Algorithms for Ordinary Differential Equations; 2nd ed.*, Springer, Dordrecht, 2006.
- [21] J. HESTHAVEN, G. ROZZA, AND B. STAMM, *Certified Reduced Basis Methods for Parametrized Partial Differential Equations*, *SpringerBriefs in Mathematics*, Springer International Publishing, 2015, <https://books.google.ch/books?id=KqtnCgAAQBAJ>.
- [22] K. ITO AND S. S. RAVINDRAN, *A reduced basis method for control problems governed by PDEs*, in *Control and estimation of distributed parameter systems (Vorau, 1996)*, Birkhäuser, Basel, 1998, pp. 153–168.
- [23] K. ITO AND S. S. RAVINDRAN, *A reduced-order method for simulation and control of fluid flows*, *Journal of Computational Physics*, 143 (1998), pp. 403–425.
- [24] K. ITO AND S. S. RAVINDRAN, *Reduced basis method for optimal control of unsteady viscous flows*, *International Journal of Computational Fluid Dynamics*, 15 (2001), pp. 97–113.
- [25] M. KAROW, D. KRESSNER, AND F. TISSEUR, *Structured eigenvalue condition numbers*, *SIAM Journal on Matrix Analysis and Applications*, 28 (2006), pp. 1052–1068 (electronic).
- [26] A. KOLMOGOROFF, *Über die beste Annäherung von Funktionen einer gegebenen Funktionenklasse*, *Annals of Mathematics. Second Series*, 37 (1936), pp. 107–110.
- [27] K. KUNISCH AND S. VOLKWEIN, *Galerkin proper orthogonal decomposition methods for a general equation in fluid dynamics*, *SIAM Journal on Numerical Analysis*, 40 (2002), pp. 492–515.
- [28] S. LALL, P. KRYSL, AND J. E. MARSDEN, *Structure-preserving model reduction for mechanical*

- 905 *systems*, Physica D: Nonlinear Phenomena, (2003).
- 906 [29] I. MARKOVSKY, *Low Rank Approximation: Algorithms, Implementation, Applications*, Springer
907 Publishing Company, Incorporated, 2011.
- 908 [30] J. E. MARSDEN AND T. S. RATIU, *Introduction to mechanics and symmetry*, vol. 17 of Texts
909 in Applied Mathematics, Springer-Verlag, New York, New York, NY, second ed., 1999.
- 910 [31] Y. MATSUO AND T. NODERA, *Block symplectic Gram-Schmidt method*, ANZIAM Journal. Elec-
911 tronic Supplement, 56 (2014), pp. C416–C430.
- 912 [32] C. MEHL, V. MEHRMANN, A. C. RAN, AND L. RODMAN, *Perturbation analysis of lagrangian
913 invariant subspaces of symplectic matrices*, Linear and Multilinear Algebra, 57 (2009),
914 pp. 141–184.
- 915 [33] V. MEHRMANN AND F. POLONI, *Doubling algorithms with permuted lagrangian graph bases*,
916 SIAM Journal on Matrix Analysis and Applications, 33 (2012), pp. 780–805.
- 917 [34] V. MEHRMANN AND F. POLONI, *An inverse-free adi algorithm for computing lagrangian invari-
918 ant subspaces*, Numerical Linear Algebra with Applications, 23 (2016), pp. 147–168.
- 919 [35] V. MEHRMANN AND D. WATKINS, *Structure-preserving methods for computing eigenpairs of
920 large sparse skew-Hamiltonian/Hamiltonian pencils*, SIAM Journal on Scientific Comput-
921 ing, 22 (2000), pp. 1905–1925 (electronic).
- 922 [36] F. NEGRI, A. MANZONI, AND D. AMSALLEM, *Efficient model reduction of parametrized systems
923 by matrix discrete empirical interpolation*, Journal of Computational Physics, 303 (2015),
924 pp. 431–454.
- 925 [37] L. PENG AND K. MOHSENI, *Symplectic Model Reduction of Hamiltonian Systems*, SIAM Journal
926 on Scientific Computing, 38 (2016), pp. A1–A27.
- 927 [38] J. S. PETERSON, *The reduced basis method for incompressible viscous flow calculations*, Society
928 for Industrial and Applied Mathematics. Journal on Scientific and Statistical Computing,
929 10 (1989), pp. 777–786.
- 930 [39] A. PINKUS, *N-widths in approximation theory*, 1985.
- 931 [40] R. V. POLYUGA AND A. VAN DER SCHAFT, *Structure preserving model reduction of port-
932 Hamiltonian systems by moment matching at infinity*, Automatica, 46 (2010), pp. 665–672.
- 933 [41] S. PRAJNA, *POD model reduction with stability guarantee*, 42nd IEEE International Conference
934 on Decision and Control, 5, pp. 5254–5258 Vol.5.
- 935 [42] A. QUARTERONI, A. MANZONI, AND F. NEGRI, *Reduced basis methods for partial differential
936 equations*, vol. 92 of Unitext, Springer, Cham, 2016.
- 937 [43] S. S. RAVINDRAN, *Adaptive reduced-order controllers for a thermal flow system using proper
938 orthogonal decomposition*, SIAM Journal on Scientific Computing, 23 (2002), pp. 1924–
939 1942 (electronic).
- 940 [44] G. ROZZA, *Reduced-basis methods for elliptic equations in sub-domains with a posteriori error
941 bounds and adaptivity*, Applied Numerical Mathematics, 55 (2005), pp. 403–424.
- 942 [45] A. SALAM AND E. AL-AIDAROUS, *Equivalence between modified symplectic gram-schmidt
943 and householder sr algorithms*, BIT Numerical Mathematics, 54 (2014), pp. 283–302,
944 doi:10.1007/s10543-013-0441-5, <http://dx.doi.org/10.1007/s10543-013-0441-5>.
- 945 [46] D. S. WATKINS, *On Hamiltonian and symplectic Lanczos processes*, Linear Algebra and its
946 Applications, 385 (2004), pp. 23–45.
- 947 [47] H. XU, *An SVD-like matrix decomposition and its applications*, Linear Algebra and its Appli-
948 cations, 368 (2003), pp. 1–24.